J Mater Sci (2008) 43:2263–2269
DOI 10.1007/s10853-007-2072-1

Chemical tuning polymorphology of functional materials by hydrothermal and solvothermal reactions

Chenglin Yan · Longjiang Zou · Dongfeng Xue · Jiasheng Xu · Meinan Liu

Received: 27 October 2006 / Accepted: 20 July 2007 / Published online: 27 September 2007

Abstract Both hydrothermal and solvothermal reactions have been employed to chemically tune the polymorphology of functional materials, such as ZnO, ZnS, $BaCO_3$, magnesium salts, copper salts, and lithium niobate. Novel self-assembled nest-like $Mg_5(CO_3)_4(OH)_2{\cdot}4H_2O$ microspheres are formed without any organic additive or catalyst. Malachite [$Cu_2(OH)_2CO_3$] with a hierarchical sphere-like architecture and lindgrenite [$Cu_3(OH)_2(MoO_4)_2$] with a hollow and pricky sphere-like architecture have been synthesized via a simple and mild hydrothermal route. Uniform hexagonal pencil-like $BaCO_3$ whiskers have been synthesized by the chemical reaction of barium chloride and urea via a facile hydrothermal route. The solvothermal route has also been successfully demonstrated to the synthesis of cube-shaped lithium niobate and complex ZnO. Our results demonstrate that hydrothermal or solvothermal reactions can be used as a versatile route to the chemical synthesis of tuning polymorphology of functional materials.

Introduction

Chemical tuning polymorphology of multiscale materials has been attracting considerable attention owing to the obvious importance of the shape and texture of materials in determining their practical properties [1–3]. Controlled synthesis of multiscale materials in terms of size and morphology has been strongly motivated by the requirements to uncover and map their size- and morphology-dependent properties and to achieve their practical applications [4–6]. As a consequence, many synthetic methods have been developed to prepare polymorphology of multiscale materials [7–11]. In particular, hydrothermal and solvothermal reactions have been regarded as one of the most effective and powerful routes to chemical synthesis of novel compounds, since it has the merits of superior composition and the wide selection of morphological controls [12–18].

Any morphology is determined by two parts, both thermodynamics and kinetics. The thermodynamics is controlled by the crystallographic characteristics of target compound, while the kinetic factor is strongly depended on our selection of chemical routes [19–21]. Generally speaking, any morphology can be separated into two stages, the nucleation and crystal growth, which should be skillfully controlled if we want to precisely perform the morphology control. Our strategy is to select dominant factors depending on crystallographic characteristics of target functional materials, such as ZnO, ZnS, $BaCO_3$, magnesium salts, copper salts, and lithium niobate to chemically tune their polymorphology with possible potential applications.

Previously, we have synthesized ZnS tetrapods [22], nanobelts [23], and the oriented assemblies of ZnS nanostructures [24] using a thermal reaction process. In our present work, a low-temperature, environmentally benign, solution-based route to multiscale ZnO with a polymorphology has been successfully demonstrated. $Zn_5(CO_3)_2(OH)_6$ precursor for ZnO is synthesized by a homogeneous precipitation reaction between zinc acetate and urea. The pyrolysis of $Zn_5(CO_3)_2(OH)_6$ precursor results in

C. Yan · L. Zou · D. Xue (✉) · J. Xu · M. Liu
State Key Laboratory of Fine Chemicals,
Department of Materials Science and Chemical Engineering,
School of Chemical Engineering, Dalian University of Technology, 158 Zhongshan Road, Dalian 116012, China
e-mail: dfxue@chem.dlut.edu.cn

microstructured and nanostructured ZnO without the morphology deformation. The controlled morphology of ZnO nanomaterials has been mainly achieved through the use of appropriate additives, such as ethylene glycol (EG) and polyethylene glycol (PEG). Furthermore, by using $Zn_5(CO_3)_2(OH)_6$ microspheres as a starting reactant and in situ template, both hollow ZnS and ZnO architectures have been successfully fabricated. We have also prepared various morphologies of magnesium salts and MgO by the reaction of $MgCl_2$ and urea, such as the novel nestlike MgO by a hierarchical self-assembly of nanosheets, MgO whiskers with a good homogeneity and high yield, MgO and $Mg(OH)_2$ nanoflowers composed of many petals, and hexagonal $Mg_5(CO_3)_4(OH)_2{\cdot}4H_2O$ micropetals. A novel spontaneous ion replacement route based on solubility difference as the driving force to a number of metal oxides has also been established for the synthesis of microstructured and nanostructured Mn_2O_3, ZnO, CuO, CdO, Al_2O_3, and CaO. Additionally, many copper compounds have been successfully fabricated with different morphologies via a solution route, such as malachite [$Cu_2(OH)CO_3$], lindgrenite [$Cu_3(OH)_2(MoO_4)_2$], and copper hydroxyphosphate [$Cu_2(OH)PO_4$] with different architectures synthesized via a simple and mild hydrothermal route in the absence of any external inorganic additives or organic structure-directing templates. By the way, the morphology control of $BaCO_3$ and $LiNbO_3$ is also successfully performed by hydrothermal or solvothermal reaction.

Experimental section

The target functional materials, such as ZnO, ZnS, $BaCO_3$, magnesium salts, copper salts, and lithium niobate had been selectively synthesized through hydrothermal or solvothermal reaction. In a typical synthesis, an appropriate amount of $MnSO_4$, $Zn(CH_3COO)_2$, $CuCl_2$, $CdSO_4$, $Al_2(SO_4)_3$, or $CaCl_2$ was dissolved in deionized water and followed by the addition of 0.002 mol $Mg_5(CO_3)_4(OH)_2{\cdot}4H_2O$ powders. HCl solution (1 M) or $NH_3{\cdot}H_2O$ (25 wt.%) solution was added into the vigorously stirred mixture to adjust pH value to the desirable one. The mixture was transferred into a Teflon-lined autoclave of 40 mL capacity. The autoclave was then filled with water up to 80% of the total volume and sealed into an electric oven and maintained at 95–180 °C for 2–24 h. All final samples were collected, filtered off, washed with deionized water and absolute ethanol several times, respectively. Finally, these samples were dried in air at 60 °C for 4 h. Mn_2O_3, ZnO, CuO, CdO, Al_2O_3, and CaO were obtained by pyrolysis of their corresponding precursors. Solvothermal reaction using ethylene glycol as solvent was employed to synthesize ZnO nanomaterials, which were synthesized through a reaction between urea and $Zn(CH_3COOH)_2$ in the ethylene/water system. In order to synthesize magnesium salts, the experiment was carried out through a hydrothermal reaction between $MgCl_2$ and urea. Similarly, hydrothermal reaction was used to synthesize copper and barium salts, and solvothermal reaction was applied to the synthesis of lithium niobate. All samples were characterized by X-ray diffraction (XRD) on a Rigaku-DMax 2400 diffractometer equipped with the graphite monochromatized Cu Kα radiation. Scanning electron microscopy (SEM) images were taken with a JEOL-5600 LV scanning electron microscope, using an accelerating voltage of 20 kV.

Results and discussion

Synthesis of binary oxides by a spontaneous ion replacement route at hydrothermal condition

The novel ion replacement approach described herein is derived from the solubility difference between two carbonate salts, in which metal cation can be driven from one liquid phase into one solid phase in the solution system. The resulting metal carbonate salts are initially formed and subsequently calcined to form high crystalline metal oxides. In a typical synthesis, $M_x(CO_3)_y(OH)_z$ (x, y, z = 0, 1, 2, 3, 4, or 5) particles are obtained by replacement of Mg^{2+} with $M^{2+,\ 3+}$ through the following reaction:

$$M^{2+,3+} + Mg_5(CO_3)_4(OH)_2(s) \leftrightarrow M_x(CO_3)_y(OH)_z(s) + Mg^{2+} \quad (1)$$

Since the K_{sp} coefficient for $Mg_5(CO_3)_4(OH)_2$ is higher than that of $M_x(CO_3)_y(OH)_z$ at the same reaction condition, which implies a tendency for the reaction to progress toward the target samples, the chemical equilibrium in Eq. 1 moves to the right side. We present a novel study on the ion replacement reaction for the synthesis of microstructured and nanostructured Mn_2O_3, ZnO, CuO, CdO, Al_2O_3, and CaO.

The morphology of all obtained metal oxides is examined by SEM measurements. SEM image of α-Mn_2O_3 cubes obtained by calcination of $MnCO_3$ has shown that they are perfect in shape, as shown in Fig. 1a. About 0.2 g of PEG is added to the initial reaction mixture for the synthesis of $MnCO_3$ cubes, while keeping the other synthetic conditions unchanged. Interestingly, the obtained cubic $MnCO_3$, as shown in Fig. 1b, is encapsulated by a cube-shaped transparent layer. It can be seen from Fig. 1c and d that polyhedral ZnO and self-assembled CuO can be effectively obtained. Figure 1e shows the typical diffraction pattern of Mn_2O_3 by the

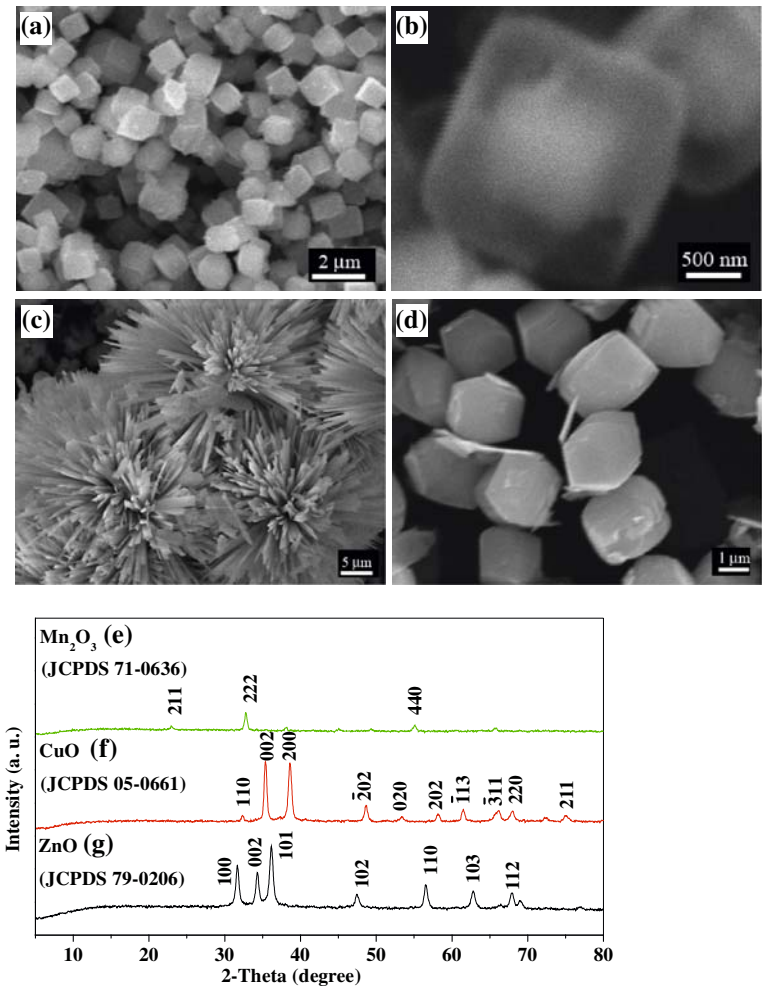

Fig. 1 SEM images and XRD patterns of metal oxides obtained by the spontaneous ion replacement reaction at hydrothermal condition: (**a**) Mn_2O_3 cubes; (**b**) $MnCO_3$ cube; (**c**) flowerlike CuO; (**d**) polyhedra ZnO; (**e**) XRD pattern of cubic phase Mn_2O_3; (**f**) XRD pattern of monoclinic phase CuO; (**g**) XRD pattern of hexagonal phase ZnO

spontaneous ion replacement of $Mg_5(CO_3)_4(OH)_2$ with Mn^{2+}, which can be readily indexed as the cubic phase α-Mn_2O_3 and the calculated cell parameter $a = 9.41$ Å, which is in a good agreement with the value in literature (JCPDS, 71-0636). Figure 1f and g shows the pure phase of monoclinic CuO (JCPDS 05-0661) and hexagonal ZnO (JCPDS 79-0206), respectively. Microstructured and nanostructured Al_2O_3, CdO, and CaO are obtained by calcination of their corresponding precursors, which are synthesized by the hydrothermal reaction of M^{2+} (M = Al, Cd, or Ca) and $Mg_5(CO_3)_4(OH)_2$. The microstructured and nanostructure characteristics of the as-prepared samples are examined by SEM measurements. SEM images in Fig. 2a–c show that spherical CdO, self-assembled CaO microrods, and spherical Al_2O_3 are successfully prepared. The compositional purity of Al_2O_3, CdO, and CaO is also confirmed by XRD, which is shown in Fig. 2. All reflections in Fig. 2d–f can be readily indexed to the hexagonal phase Al_2O_3 (JCPDS 10-0173), cubic phase CdO (JCPDS 75-1529), and cubic phase CaO (JCPDS 48-1467). The results are in a good agreement with those reported in literature, which have proven the successful synthesis of these metal oxides.

Hydrothermal and solvothermal synthesis of ZnO

A low-temperature, environmentally benign, solution-based route to multiscale ZnO with a polymorphology has also been successfully demonstrated through a solvothermal reaction. $Zn_5(CO_3)_2(OH)_6$ precursor for ZnO is synthesized by a homogeneous precipitation reaction between zinc acetate and urea. The pyrolysis of $Zn_5(CO_3)_2(OH)_6$ precursor results in microstructured and nanostructured ZnO without the morphology deformation. Figure 3 shows SEM images of $Zn_5(CO_3)_2(OH)_6$ precursor synthesized by a homogeneous precipitation reaction between zinc acetate and urea in the presence of EG or PEG. Figure 3a and b shows that the spherical $Zn_5(CO_3)_2(OH)_6$ composed of rods or cubes are synthesized in the presence of EG. Polyhedral $Zn_5(CO_3)_2(OH)_6$ precursor is synthesized in the presence of PEG, which is shown in

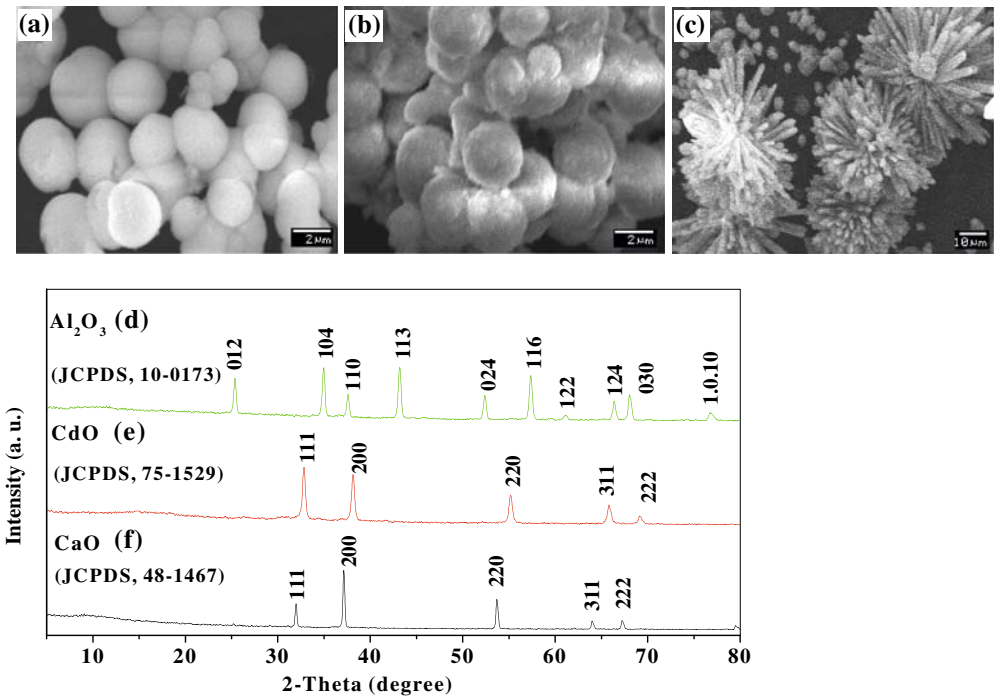

Fig. 2 SEM images and XRD patterns of metal oxides obtained by the spontaneous ion replacement reaction at hydrothermal condition: (**a**) spherical Al_2O_3; (**b**) spherical CdO; (**c**) flowerlike CaO; (**d**) XRD pattern of hexagonal phase Al_2O_3; (**e**) XRD pattern of cubic phase CdO; (**f**) XRD pattern of cubic phase CaO

Fig. 3c. All $Zn_5(CO_3)_2(OH)_6$ precursors can be converted into target ZnO with the similar morphology of ZnO, without the morphology deformation. In addition, Hollow ZnO spheres have been successfully synthesize by employing $Zn_5(CO_3)_2(OH)_6$ sphere as the sacrifice template, which is shown in Fig. 3d.

Hydrothermal synthesis of magnesium and copper salts

A novel self-assembled microstructure of nestlike $Mg_5(CO_3)_4(OH)_2{\cdot}4H_2O$ microspheres (Fig. 4a) is formed by a self-assembly of nanosheets through the hydrothermal reaction between $MgCl_2$ and urea, without any surfactant

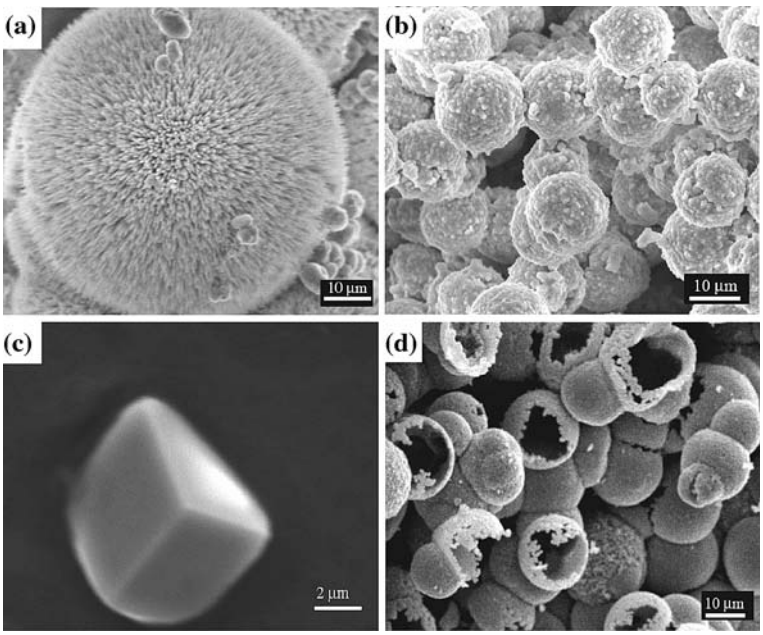

Fig. 3 SEM images of $Zn_5(CO_3)_2(OH)_6$ precursor and ZnO: (**a** and **b**) spherical $Zn_5(CO_3)_2(OH)_6$ precursor via the hydrothermal reaction in the presence of EG; (**c**) polyhedron $Zn_5(CO_3)_2(OH)_6$ precursor via the hydrothermal reaction in the presence of PEG; (**d**) hollow ZnO obtained by employing $Zn_5(CO_3)_2(OH)_6$ spheres as the sacrifice template

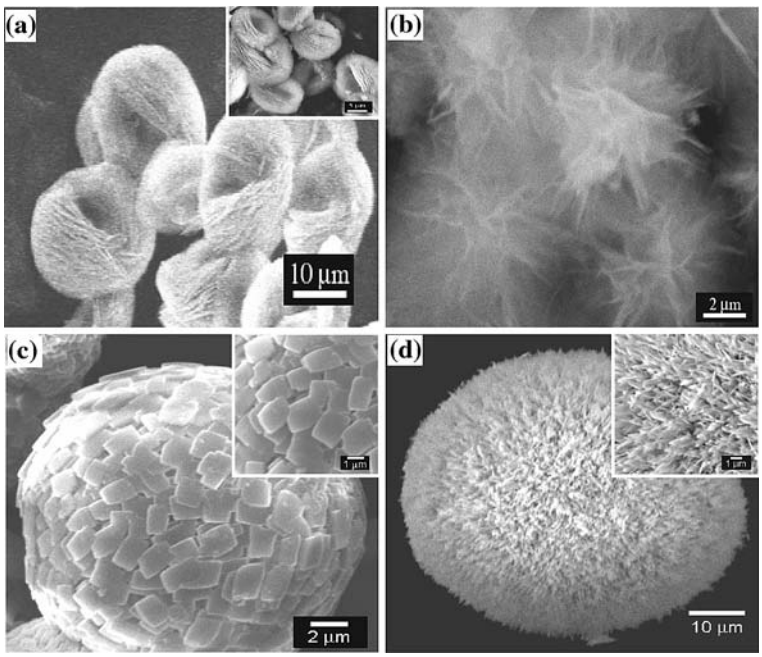

Fig. 4 (**a**) SEM image of nestlike $Mg_5(CO_3)_4(OH)_2$, inset is SEM image of nestlike MgO by calcination of the nestlike $Mg_5(CO_3)_4(OH)_2{\cdot}4H_2O$. (**b**) SEM image of $Mg(OH)_2$ nanoflowers. (**c**) SEM image of malachite architecture prepared at 110 °C and 12 h, inset is an enlarged image. (**d**). SEM image of hollow and pricky lindgrenite microspheres prepared at 110 °C and 12 h, inset is an enlarged image

or catalyst. MgO with the similar morphology (inset of Fig. 4a) can be formed by the thermal decomposition of nestlike $Mg_5(CO_3)_4(OH)_2{\cdot}4H_2O$. $Mg(OH)_2$ nanoflowers have also been obtained via a mild reaction condition, which are shown in Fig. 4b. Malachite $[Cu_2(OH)_2CO_3]$ with a hierarchical sphere-like architecture has been synthesized via a simple and mild hydrothermal route (between $CuSO_4$ and K_2CO_3) in the absence of any external inorganic additives or organic structure-directing templates. As shown in Fig. 4c, the hierarchical malachite particles, which are comprised of numerous two-dimensional micro-platelets paralleling to the sphere surface are uniform spheres with a diameter of 10–20 μm. The initial concentration of reagents, the hydrothermal reaction time and temperature are important factors, which dominantly affect the evolution of crystal morphologies. The growth of the hierarchical architecture is believed to be a layer-by-layer growth process. Further, copper oxide with the similar morphology can be easily obtained from the as-prepared malachite. In addition, lindgrenite $[Cu_3(OH)_2(MoO_4)_2]$ with a hollow and pricky sphere-like architecture has been synthesized via a simple and mild hydrothermal reaction between Cu^{2+} and Na_2MoO_4. As shown in Fig. 4d, the hierarchical lindgrenite particles are uniformly hollow and pricky spheres, which are comprised of numerous small crystal strips that are aligned perpendicularly to the spherical surface. Two factors weigh heavily in favor of the formation of hollow and pricky architecture in the present process. One is the general phenomenon of Ostwald ripening in solution, which can be responsible for the hollow structure; the other is that lindgrenite crystals have a rhombic growth habit, which plays an important role in the formation of pricky surface. Furthermore, $Cu_3Mo_2O_9$ with a similar size and morphology can be easily obtained by a simple thermal treatment of the as-prepared lindgrenite in atmosphere.

Copper hydroxyphosphate $[Cu_2(OH)PO_4]$ crystals (see Fig. 5) has been successfully synthesized through a simple and mild hydrothermal route (between $Cu(CH_3COO)_2$ and $(NH_4)_2HPO_4$) in the absence of any external inorganic additives or organic structure-directing templates. On the basis of structure and chemical bond analysis, copper hydroxyphosphate crystals tend to grow along the *c*-axis and have a rotation twinned-crystal growth habit, which is essential for the formation of various complex architectures. This hydrothermal approach provides a facile strategy to synthesize copper hydroxyphosphate crystals with unique morphologies and complex architectures, which may be applicable to the synthesis of other inorganic materials.

Hydrothermal synthesis of $BaCO_3$ whiskers

Uniform hexagonal pencil-like $BaCO_3$ whiskers (see Fig. 6a) have been synthesized by the chemical reaction of barium chloride and urea via a facile hydrothermal route. Most whiskers have well-defined crystallographic facets and a regular prismatic hexagon with the length up to 50 μm and diameter around 5 μm. The straight pencil-like $BaCO_3$ whisker is grown along the *c*-axial direction, and the six faces of whiskers are consisted of both {010} and

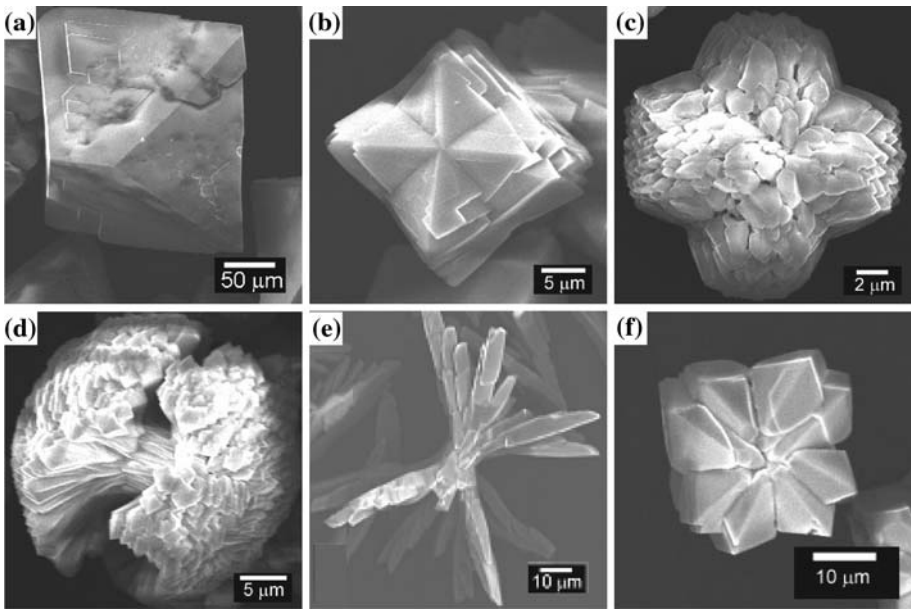

Fig. 5 SEM images of various copper hydroxyphosphate architectures: (**a**) a single crystal. (**b**) a rotation twinned-crystal; (**c**) a quadruple petal pumpkin-like architecture; (**d**) a dumbbell-shaped copper hydroxyphosphate architecture; (**e**) a double-flower-like architecture; (**f**) a well-defined aggregate

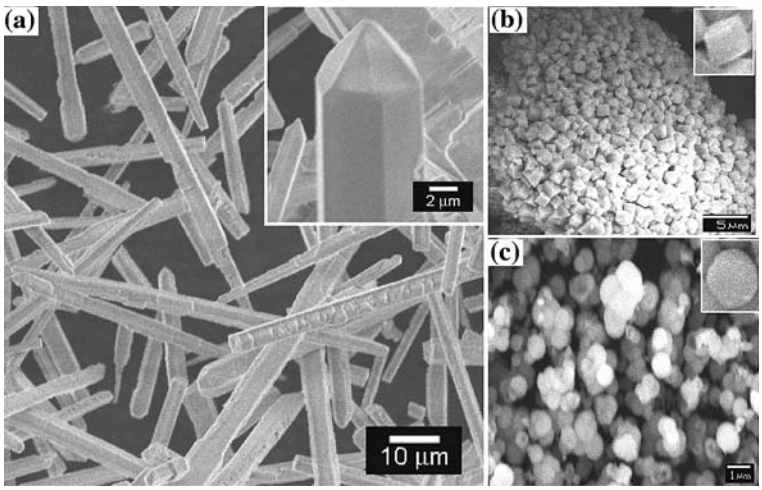

Fig. 6 (**a**) SEM images of hexagonal pencil-like $BaCO_3$ whiskers; (**b**) SEM image of the cubic $LiNbO_3$ particles; (**c**) SEM image of spherical $LiNbO_3$ particles. The upper right inset show enlarged SEM image of the corresponding particle

{110} planes. Our present hydrothermal synthetic system tends to provide an appropriate chemical microenvironment for the formation of hexagonal pencil-like $BaCO_3$ whiskers, due to the fact that the homogeneous decomposition of urea plays an essential role in the whole hydrothermal process.

Solvothermal synthesis of $LiNbO_3$

Up to now, lithium niobate powders have been successfully synthesized by several methods, such as solid-state method, combustion method [25–27], sol–gel method [28], and solvothermal method [29, 30]. In our current work, lithium niobate crystalline with a uniform cubic morphology (see Fig. 6b) has been successfully synthesized by a facile hydrothermal method (between LiOH and Nb_2O_5) in the absence of any surfactants. In the synthesis process, oxalic acid was employed as the solvent, which plays an important role since it coordinates with niobium oxide to decrease the activation energy of the system. By tuning pH of this reaction system, lithium niobate powders in a uniformly spherical shape are also successfully obtained (see Fig. 6c). An overview image at low magnification illustrates that the obtained samples are quite uniform in shape and have a spherical morphology. A closer examination of these samples indicates that the surface of those spheres is smooth and the spherical diameter is around 1 μm. The as-synthesized lithium niobate cubes and spheres may have better in optical and electric devices due to their uniform morphologies.

Conclusion

Our present work clearly shows that hydrothermal or solvothermal reactions have been regarded as one of the most effective and powerful routes to the preparation of functional materials, especially for those with strong or specific purposes, since they have the merits of superior composition and the wide selection of morphology control strategies. Therefore, in the present work, both hydrothermal and solvothermal reactions have been effectively employed to tune the polymorphology of our respective target functional materials. Reaction temperature, pH value, and solvent are important factors in determining the morphology of such samples as copper hydroxyphosphate and lithium niobate during our designed reaction systems. Our results demonstrate that hydrothermal or solvothermal reactions can be used as a versatile route to the synthesis of other inorganic materials.

Acknowledgements We gratefully acknowledge the financial support of the program for New Century Excellent Talents in University (Grant No. NCET-05-0278), the National Natural Science Foundation of China (Grant No. 20471012), a Foundation for the Author of National Excellent Doctoral Dissertation of P. R. China (Grant No. 200322), the Research Fund for the Doctoral Program of Higher Education (Grant No. 20040141004) and the Scientific Research Foundation for the Returned Overseas Chinese Scholars, State Education Ministry.

References

1. Law M, Greene LE, Goldberger J, Johnson JC, Saykally RJ, Yang P (2005) Nat Mater 4:455
2. Xu J, Xue D (2007) Acta Mater 55:2397
3. Sun Y, Xia Y (2002) Science 298:2176
4. Zhang WX, Wen XG, Yang SH, Berta Y, Wang ZL (2003) Adv Mater 15:822
5. Wang X, Gao P, Li J, Summers CJ, Wang ZL (2002) Adv Mater 14:1732
6. Li YB, Bando Y, Golberg D (2003) Adv Mater 15:581
7. Kong XY, Wang ZL (2003) Nano Lett 3:1625
8. Yan C, Xue D (2007) Electrochem Commun 9:1247
9. Yan C, Xue D (2006) J Phys Chem B 110:25850
10. Polleux J, Gurlo A, Barsan N, Weiman U, Antonietti M, Niederberger M (2006) Angew Chem Int Ed 45:261
11. Zhang H, Wang D, Mohwald H (2006) Angew Chem Int Ed 45:748
12. Yan C, Xue D (2005) J Phys Chem B 109:12358
13. Yan C, Xue D (2006) J Phys Chem B 110:7102
14. Yan C, Xue D (2006) J Phys Chem B 110:11076
15. Yan C, Xue D (2006) J Phys Chem B 110:1581
16. Yan C, Xue D, Zou L, Yan X, Wang W (2005) J Cryst Growth 282:448
17. Yan C, Xue D, Zou L (2006) Mater Res Bull 41:2341
18. Yan C, Xue D (2007) J Alloy Compd 431:241
19. Xu J, Xue D (2005) J Phys Chem B 109:17157
20. Xu J, Xue D (2006) J Phys Chem B 110:11232
21. Xu J, Xue D (2006) J Phys Chem Solids 67:1427
22. Zhu Y, Bando Y, Xue D, Golberg D (2003) J Am Chem Soc 125:16196
23. Zhu Y, Bando Y, Xue D, Golberg D (2003) Appl Phys Lett 82:1769
24. Zhu Y, Bando Y, Xue D, Golberg D (2004) Adv Mater 16:831
25. Liu M, Xue D, Zhang S, Zhu H, Wang J, Kitamura K (2005) Mater Lett 59:1095
26. Liu M, Xue D (2006) Solid State Ionics 177:275
27. Liu M, Xue D, Luo C (2006) J Am Ceram Soc 89:1551
28. Zeng HC, Tung SK (1996) Chem Mater 8:2667
29. Niederberger M, Pinna N, Polleux J, Antonietti M (2004) Angew Chem Int Ed 43:2270
30. Liu M, Xue D (2005) Mater Lett 59:2908